Constrained Waveform Inversion of Colocated VSP and Surface Seismic Data

B.R. Smithyman[*], B. Peters[†] and F.J. Herrmann[†]
[*]University of Western Ontario, [†]University of British Columbia

Abstract

Constrained Full-Waveform Inversion (FWI) is applied to produce a high-resolution velocity model from both Vertical Seismic Profiling (VSP) and surface seismic data. The case study comes from the Permian Basin in Texas, USA. This dataset motivates and tests several new developments in methodology that enable recovery of model results that sit within multiple a priori constraint sets. These constraints are imposed through a Projected Quasi-Newton (PQN) approach, wherein the projection set is the intersection of physical property bounds and anisotropic wavenumber filtering. This enables the method to recover geologically-reasonable models while preserving the fast model convergence offered by a quasi-Newton optimization scheme like l-BFGS. In the Permian Basin example, low-frequency data from both arrays are inverted together and regularized by this projection approach. Careful choice of the constraint sets is possible without requiring tradeoff parameters as in a quadratic penalty approach to regularization. Multiple 2D FWI results are combined to produce an interpolated 3D model that is consistent with the models from migration velocity analysis and VSP processing, while offering improved resolution and illumination of features from both datasets.

Introduction

Full-Waveform Inversion (FWI) is applied to generate a high-resolution model of P-wave velocity for a site in the Permian Basin, Texas, USA. New tools for FWI were motivated and tested by a field-data case study that involved the joint full-waveform inversion of data from a 3-D Vertical Seismic Profiling (VSP) survey and those from a 3-D seismic reflection (Multichannel Seismic; MCS) survey located at the same site, which shared common source Vibration Points (VPs). The resulting velocity model captures features that were not resolvable by conventional velocity analysis.

The field data for this study come from a dataset that was acquired by Vecta Oil and Gas to image Lower Paleozoic transpressional pop-up structures in the Permian Basin of Texas, USA. The dataset was recorded in 2010 and contains seismic waveforms from a 3-D VSP survey comprising 151 downhole 3-component geophones and a 3-D seismic reflection survey comprising 1649 vertically-polarised geophones (see Figure 1). The joint inversion of the MCS and VSP datasets results in equivalent but separate processing steps at several stages of the inversion. A number of practical choices are made to improve the tractability of the FWI problem. In the current approach, several 2-D cross-sectional slices are processed by independent 2-D FWI in this study, though the resulting models are assessed together; these separate FWI problems use appropriate subsets of the sources and receivers from the 3-D survey, and do not share data or depend on each other directly. Both surveys shared a common source array, with 2785 shared surface vibroseis sources. The frequency content of the source vibroseis sweep ranged from 8–120 Hz, which constrained the minimum frequency for FWI. The surface and downhole geophones were critically damped above 10 Hz and 15 Hz, respectively. This results in a practical starting frequency for FWI of 8 Hz, with maximal Signal to Noise Ratio (SNR) at about 10 Hz. FWI processing used 32 frequencies from 8.00 to 15.75 Hz. The 151 downhole receivers are positioned from 1284 m to 3569 m depth at 15 m intervals. The surface sources and receivers are positioned in concentric circles surrounding the VSP well head (Figure 1). From the 3-D survey, a series of 2-D cross-sectional lines may be extracted that intersect the VSP well, resulting in a 2D joint survey geometry that includes data from several sources and surface receivers, as well as all 151 downhole geophones. Two baseline models are available from separate seismic contractors, the first of which acts as the initial model for FWI in this study. (1) A smooth 3-D velocity model was developed during by 3-D Migration Velocity Analysis (MVA) during Pre-Stack Depth Migration (PSDM) processing (see Figure 2a). The initial migrated image provided sufficient detail to focus reflectors effectively to middle depths, but lensing through high-velocity carbonate rocks at 1200–2700 m depth resulted in mis-migration at reservoir depths. This motivates full-waveform processing to improve the quality of the velocity model. (2) A 2-D velocity model (Figure 2b) is available that is based on extrapolation of a 1-D vertical velocity profile from processing of

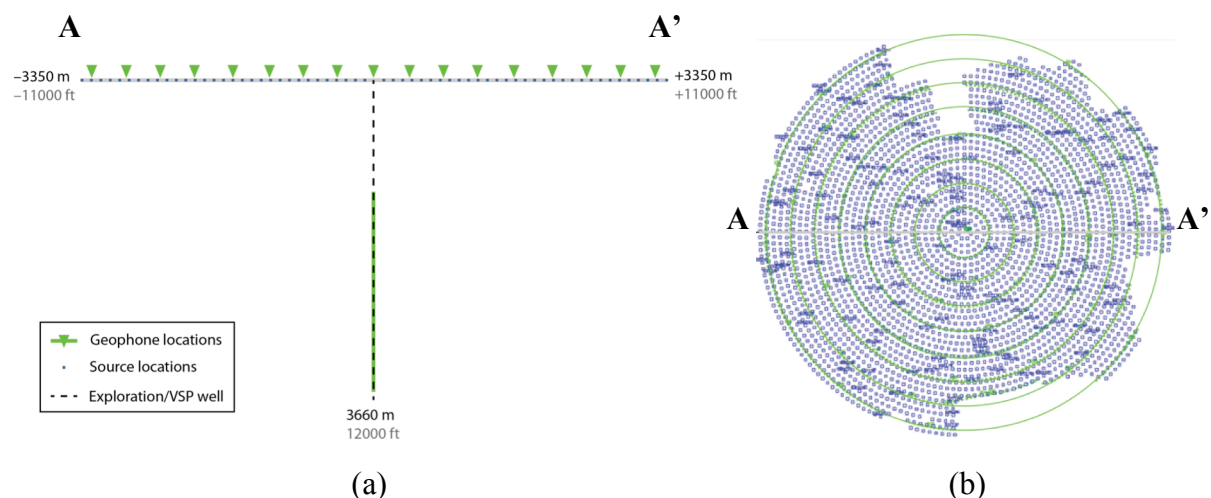

(a)   (b)

Figure 1 Survey geometry is indicated in (a) cross-sectional view and (b) plan-view. The vibroseis sources (shown in blue) and surface geophones (green) are deployed in concentric rings. The downwell geophones are cemented at 15 m intervals beginning at 1284 m depth.

VSP data. The starting model for full-waveform inversion (Figure 2a) is derived from the 3-D model originally produced during migration velocity analysis (MVA), which is broadly similar to a low-wavenumber version of the VSP velocity profile (Figure 2b); however, the MVA velocity model possesses smoothly-varying 3-D structures that are not fully accounted for in 2-D processing. An initial model for 2-D full-waveform inversion is produced by slicing the 3-D velocity volume from MVA and extracting a 2-D slice at an arbitrary north asimuth, intersecting the well. This abstract focuses on results from an E–W cross-section (Figure 1a, Figure 2a–c).

Method

Full-waveform inversion is a nonlinear process by which an Earth model is iteratively updated to better predict recorded field seismograms. The FWI procedure we follow herein is based on Herrmann et al. (2013) and Pratt (1999), but with several adaptations to enable the processing of 3-D on-land field data using a 2-D acoustic FWI code. We use a recently introduced optimization and regularization framework as described in detail by Schmidt et al. (2009). The numerical implementation is developed in Parallel MatLab and allows for parallelism over frequencies. The seismograms measured in the field are the result of waves propagating in 3-D through a complex elastic earth, whereas the simulated seismograms from our method represent solutions to the 2-D constant-density Helmholtz equation. The discrete implementation uses Perfectly Matched Layer (PML) boundary conditions on all sides of the model, and the inversion procedure updates the model of squared slowness, $m = 1/\mathbf{c}^2$, wherein $\mathbf{c}$ is acoustic velocity. Sources and receivers are modelled using approximate vertical dipoles, in order to account very approximately for the radiation patterns of vibroseis sources and vertically-polarised geophones. The source signature is estimated by Newton search and a separate calibration factor is found for each array (MCS and VSP) at each stage of inversion. The bulk Amplitude Variation with Offset (AVO) characteristics of the medium are scaled to account partially for the differing geometric spreading patterns between the 3-D elastic Earth and the 2-D acoustic medium that is modelled. This is accommodated by a log-linear AVO scale factor (see Brenders and Pratt, 2007) for each array, prior to joint inversion.

The joint inversion of data from multiple arrays makes regularization on model parameters necessary to promote the recovery of geologically-meaningful results. Regularization implies the incorporation of *a priori* information into the recovered earth models. In this study, regularization is accomplished by constraining the inversion to only return model iterates that fit some criteria by projection onto a constraint set, which is discussed in another submission to these proceedings by Peters, Smithyman and Herrmann. The optimization problem is solved by Projected Quasi-Newton (PQN) method (Schmidt et al., 2009), which solves the constrained optimization problem such that the data misfit is minimal. The model is made consistent with the regularization term by application of the projection operator prior to full-waveform inversion. The constraint set has two criteria: (1) Its support in the 2D wavenumber domain is restricted to an elliptical region surrounding the zero wavenumber; i.e., a 2D low-pass filter that may allow for anisotropic smoothing. The projection operator takes the form $\mathcal{P} = \mathbf{E}^T\mathbf{F}^T\mathbf{S}\mathbf{F}\mathbf{E}$ wherein $\mathbf{E}$ is a 2D mirror-extension operator, $\mathbf{F}$ is the 2D discrete Fourier transform, and $\mathbf{S}$ is a diagonal matrix selecting filter coefficients. (2) Model velocities ($\mathbf{c}$) are bounded pointwise to be within $1500 \leq \mathbf{c} \leq 7000$. These two criteria are composed to produce a constraint set that may be enforced through Dykstra's projection algorithm, which projects the model vector onto the edge of the intersection set that satisfies both criteria. The filter coefficients for the construction of $\mathbf{S}$ (and therefore, $\mathcal{P}$) are chosen adaptively, such that the vertical wavenumbers in the model are limited above a scaled threshold $k_{\max} = \omega_{\max}/c_{\min}$ at each iteration, where $k_{\max}$ is the target maximum vertical wavenumber, $\omega_{\max}$ is the maximum frequency and $c_{\min}$ is the minimum P-wave velocity. The horizontal wavenumber limit is chosen in terms of some ratio to the vertical wavenumber limit (in this case 5:1) in order to encourage models that exhibit strong horizontal smoothness; this is representative of the expected structures in a sedimentary basin such as the Permian Basin. The value of $k_{\min}$ is adapted based on the temporal frequencies included at each stage of the FWI procedure; hence, structures in the model are tied to some proportion of the theoretical resolving power of the FWI sensitivity kernel (Brenders and Pratt, 2007) for the maximum frequency at each iteration.
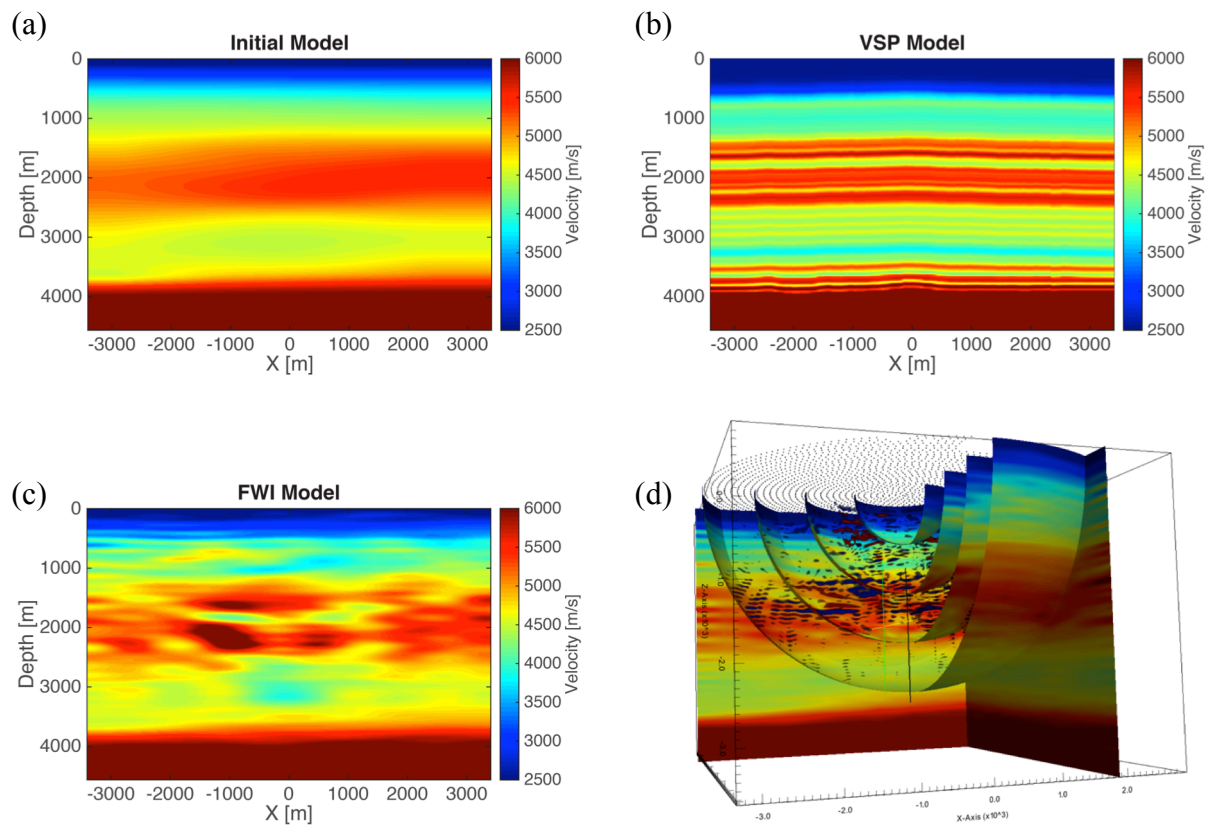
(a) Initial Model

(b) VSP Model

(c) FWI Model

(d)

Figure 2 *Model results are shown from full-waveform inversion processing. (a) Initial model from PSDM contractor, extracted from 3-D MVA velocity volume. (b) VSP model from contractor; not used in FWI processing, but shown for comparison purposes. (c) Velocity model resulting from full-waveform inversion processing in 2-D E–W cross-section. (d) Sliced volume from 3-D composite FWI result, produced by interpolation of eight 2-D results at 22.5° intervals in North asimuth.*

Results

Because the accurate modelling of the physics is highly dependent on the initial velocity model, a poor choice of initial model will cause the inversion to converge towards a local minimum of the objective function (Shah et al., 2010; Pratt, 1999). We therefore assess the initial data misfit for both datasets considered by joint inversion (see Figure 3a and 3c). Particular attention is paid to the phase misfit, which depends strongly on the kinematics of the waves and may be examined to determine whether the model under- or over-predicts traveltimes by more than one half cycle. If the phase misfit for given source/receiver pair is larger than a half cycle then the FWI process may converge towards a local minimum of the objective function (Shah et al., 2010). Examination of the data misfit for the downhole receivers in the initial velocity model (Figure 2a) indicates that the phase residuals are less than one half cycle (i.e., $\pm\pi$) within about 2.5 km of the centre of the model for the downwell array (sources 10–50), and within about 1.5–2.0 km of the centre of the model for the surface array (see Figure 3a and 3c). However, because the surface receivers are sampled coarsely (~402 m), it is difficult to confirm whether cycle skips are present in residuals for the MCS array (e.g., by visual artefacts; see Shah et al., 2010). The data misfit is also assessed for the FWI result, presented in Figure 3b and 3d. The phase and amplitude misfits are both substantially reduced in the low-frequency and high-frequency panels, although the source locations at the outermost rings of the surface array continue to show higher phase residuals that could indicate cycle skips at the sides of the array. The misfit images are unfortunately dominated by surface-consistent timing errors (cross-hatched patterns) at the highest frequency of 15.75 Hz, but the bulk change in the residuals is similar to 8.75 Hz. The final FWI result (Figure 2c) shows improved resolution and images layered structures that are believed to exist in the centre of the survey area, based on comparison with the model from VSP processing (Figure 2b). Confidence in this model is lower on the left and right flanks, based on
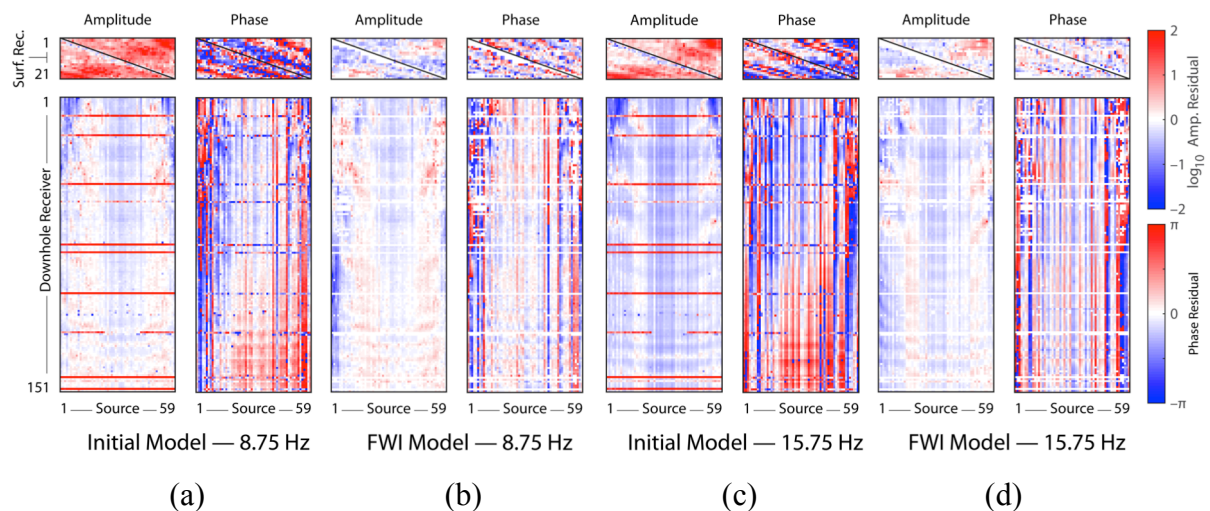
Figure 3 *Data comparison, showing amplitude and phase residuals for four cases. (a) Initial model at 8.75 Hz; compare with (b) FWI model at 8.75 Hz. Phase and amplitude residuals are substantially reduced. (c) Initial model at 15.75 Hz; compare with (d) FWI model at 15.75 Hz. Data misfits are reduced at 15.75 Hz (particularly for surface data), but whereas the smoothly varying component of the residual is reduced substantially, the data misfit is dominated by surface-consistent timing errors.*

analysis of the data residuals, though regularization avoids extreme model artefacts. Results from multiple 2-D sub-problems are combined to produce a 3-D velocity model that is useful for interpreting structures at this site (Figure 3d). Ongoing work involves: 1) pursuing 3-D FWI processing using a fully 3D code to treat the model and data in the domain that is most appropriate; 2) examining the effects of mild anisotropy at middle depths; and 3) re-migration of surface seismic data using the improved velocity model from FWI.

Acknowledgments

References

Brenders, A. and Pratt, R.G. [2007] Full waveform tomography for lithospheric imaging: Results from a blind test in a realistic crustal model. *Geophysical Journal International*, **168**, 133–151.

Herrmann, F.J., Hanlon, I., Kumar, R., van Leeuwen, T., Li, X., Smithyman, B., Wason, H., Calvert, A.J., Javanmehri, M., Takougang, E.T. [2013] Frugal full-waveform inversion: From theory to a practical algorithm. *The Leading Edge*, **32** (9), 1082–1092.

Pratt, R.G. [1999] Seismic waveform inversion in the frequency domain, Part 1: Theory and verification in a physical scale model. *Geophysics*, **64** (3), 888–901.

Schmidt, M., van den Berg, E., Friedlander, M. and Murphy, K. [2009] Optimizing costly functions with simple constraints: A limited-memory projected quasi-newton algorithm. *JMLR*, **5**, 456–463.

Shah, N., Warner, M., Guasch, L., Stekl, I. and Umpleby, A. [2010] A strategy for waveform inversion without an accurate starting model. 72nd *EAGE Conference Barcelona*.